BULLETIN
OF THE
KOREAN CHEMICAL SOCIETY

VOLUME 15, NUMBER 10
OCTOBER 20, 1994

BKCS 15(10) 811-916
ISSN 0253-2964

Communications

Determination of Trace Methane Impurities in Ultra-High Purity Gases by Gas Chromatography

Byung Ryul Rho, Byung Eon Park, Doo Seon Park*, and Moo Ryong Son

Daesung Cryogenic Research Institute, Daesung Sanso Co., Ltd. Ansan, 425-090, Korea

Received January 31, 1994

As the ultra-large scale integration(ULSI) of the semiconductor devices,[1,2] it is very important to accurately measure trace impurities in ultra-high purity (UHP) gases at levels as low as a few ppb. Correspondingly, analytical methods such as Atmospheric Pressure Ionization Mass Spectrometry (APIMS) have been developed to determine the ppb level concentration.[3,4] Even though the APIMS has a tremendous analytical power, it has not been widely used because of its considerable cost to the user in terms of equipment expense and its complexity. In this regard, GC represents the most commonly used method in the gas analysis,[5] especially, GC-FID is very useful as an analytical tool for UHP gases because of its high sensitivity for hydrocarbon impurities, simplicity and wide linear range. The response of FID for methane is directly proportional to its concentration over a wide region. The linear range of a detector may be defined as the ratio of the largest to the smallest impurity concentration within which the detector is linear. The linear limits of the FID[6] is, by definition, between 10^6 and 10^7.

Up to now, an analysis of hydrocarbon impurities has scarcely ever been reported at low ppb levels by GC-FID. It is considered that hydrocarbon impurities are difficult to determine in the low ppb level ($\leq$10 ppb) by GC-FID. It is known that the limit of detection (LOD) of the FID for methane is *ca.* 10 ppb[7]. However, trace impurity levels at less than 10ppb can be measured by the use of a newly-developed data processor. Additionally, the peak areas arising from trace impurities can be easily calculated and identified by the data processor's zooming function. It goes without saying that a calibration system, in well-controlled manner, is indispensable to find the trace impurities as low as a few ppb.

In this study, trace methane impurity in UHP gases is determined by GC-FID at low ppb levels. Main concern in the present work is to know the LOD of the FID for methane.

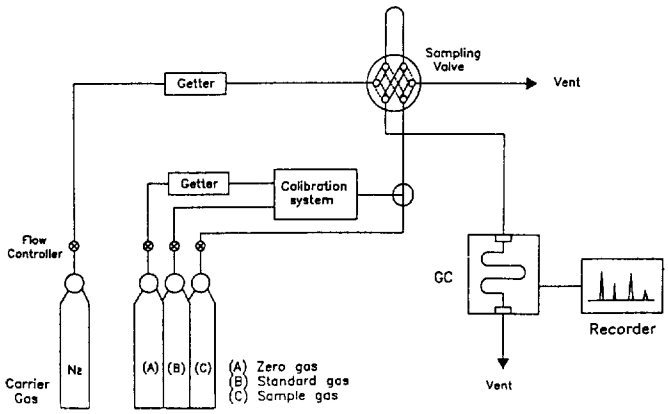

Figure 1. Schematic diagram of the experimental apparatus.

Experimental

The schematic diagram of the experimental apparatus is shown in Figure 1. All components such as tubing, fittings, and valves used in the apparatus are SUS316L stainless steel. The N_2 carrier gas (99.9999%) is purified by a getter (Saes getters S.P.A., Model GC50). The GC-FID employed in the experiment is the Shimadzu Model GC-14BPTF gas chromatograph with a data processor (Model C-R7A). The sample gas is introduced by the Shimadzu MGS-5 gas sampling valve. The operational conditions of the GC are illustrated in Table 1.

The calibration is performed using a standard addition technique.[8] A getter is also used for purification of the zero gas. The calibration gas contains several-ppm-level impurity. The mass flow controllers(MFC, Aera Co., Japan, Model FC 770AC) employed in the calibration system are calibrated by a soap bubble flow-meter for each gas. The schematic

*To whom correspondence should be addressed.

Table 1. Operational conditions of column and detector

Column: Activated Alumuina 80/100 mesh, 3mm I.D.×2m length
Column temperature: 35℃
Detector: FID
Detector temperature: 200℃
Range: 10^1, 10^0
Sample loop: 1 ml
Carrier gas: 30 ml/min

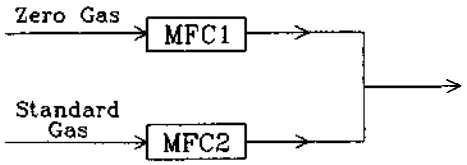

Figure 2. Schematic diagram of the calibration system.

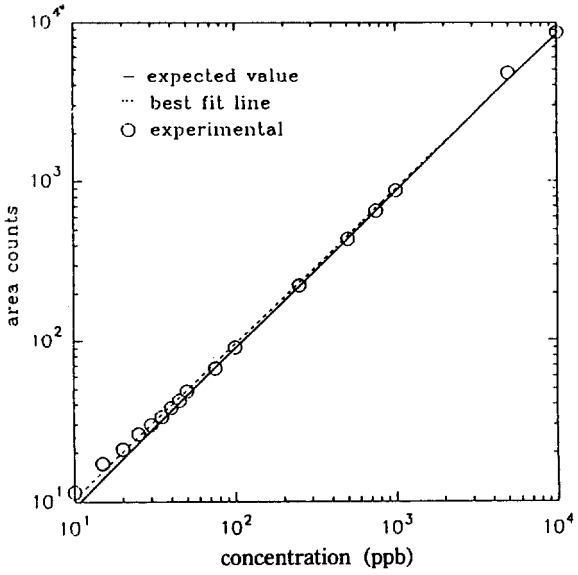

Figure 3. Area counts *vs.* methane impurity addition to the zero gas.

diagram of the calibration system is shown in Figure 2. The blending ratio varies in the range of 1,000 to 1 by adjusting the flowrates of the MFC's.

Results and Discussion

Calibration. Figure 3 shows the area counts plotted against the concentration of methane. The sampling loop used is 1 ml volume. The calibration curve for methane in nitrogen presents a good linearity over a wide range of 10 to 10^4 ppb. Each data point in Figure 3 is the average of five measurements. The solid line is the expected value by blending sample. The dashed one is the best fit line obtained from a linear regression analysis. The open circles are experimental results. In the lower concentration limits, the experimental data are a little larger than expected values. In this region, if the blending ratio is too large, the

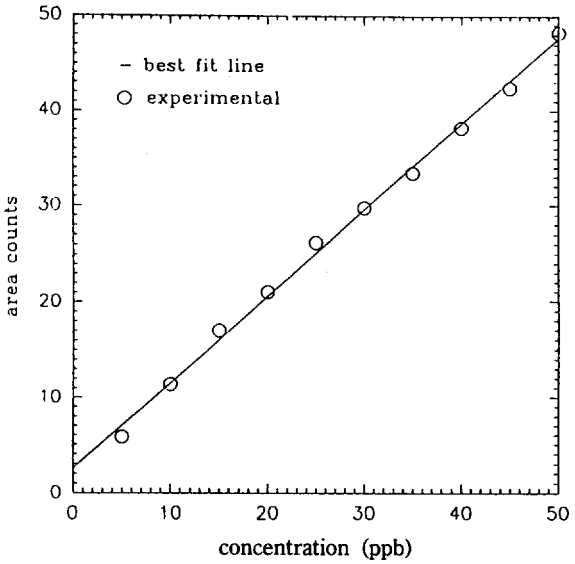

Figure 4. Methane calibration curve.

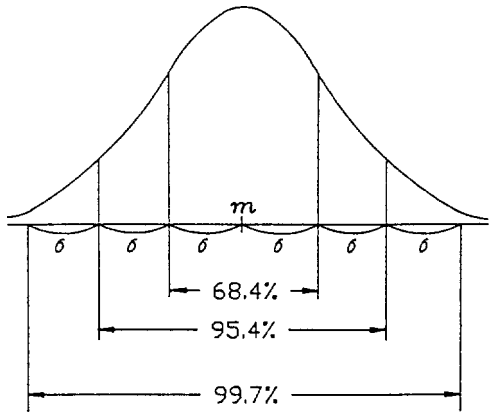

Figure 5. Normal distribution.

obtained data go off the true values. In orther words, this calibration becomes nonlinear at concentrations below 50 ppb. In order to raise the accuracy of measurements, it is desirable to use a standard sample containing less than 1 ppm. Therefore, an intermediate standardized sample of 0.7 ppm methane subsequently is utilized in order to obtain the necessary calibration data in the lower concentration range of 5 to 50 ppb. The results are shown in Figure 4.

As shown in Figure 4, the solid line is the best fit one by linear regression analysis of calibration data. Generally, the lower concentration region, the bigger experimental errors. In this work, however, the calibration curve shows a good linearity in the concentration range of 5 to 50 ppb.

Detection Limits. There are many published LOD definitions.[9-11] In this work, International Union of Pure and Applied Chemistry (IUPAC) definition was employed.[8] The IUPAC definition adopted 3-sigma(3 standard deviation)rule.

In a certain range of concentration, the instrument response is linear with respect to concentration and yields calibration curve with an equation of the following form:

$$y = mx + i \quad (1)$$

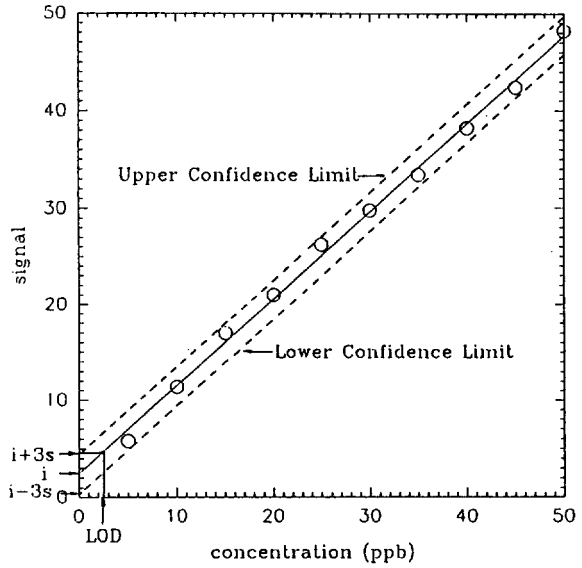

Figure 6. LOD determination by 3-sigma rule.

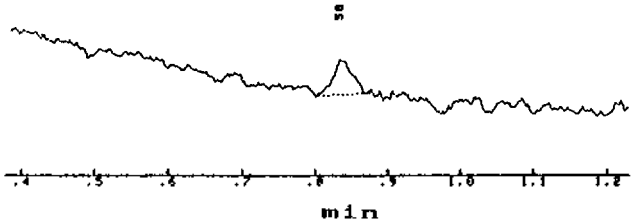

Figure 7. Chromatogram of 5 ppb of methane impurity addition to the zero gas.

Where y is the instrument response, x is the concentration of added impurity, m is the analytical sensitivity which can be obtained from the slope of the calibration curve, and i is the intercept. The IUPAC definition expresses the LOD as follows:

$$\text{LOD} = 3S_b/m \quad (2)$$

Here, S_b is the standard deviation of the blank. It is determined experimentally. And also, it can be expressed in terms of s, sample standard deviation. The standard deviation, s or , σ is obtained from linear regression analysis of calibration data.

In a normal distribution, as shown in Figure 5, most of the data(99.7%) are in the range of $m-3\sigma$ to $m+3\sigma$. Here, m is the mean value.[12] It has the exactly same meaning as i in Figure 6. In the concentration range of 5 to 50 ppb, there are most calibration data between the upper and lower confidence level as shown in Figure 6. The sample standard deviation, s, the slope of the calibration curve, m, and the intercept(mean value), i, obtained from linear regression analysis of the calibration data are 0.72, 0.9 and 2.6, respectively. From the above results, the LOD of the FID for methane is ca. 2.4 ppb.

Actually, the area counts corresponding to 5 ppb of methane in nitrogen is conspicuous as shown in Figure 7. The larger the sample loop, the bigger the peak.

Analyses of UHP Gases. Figure 8 shows chromatograms of UHP gases produced by DSSC. All chromatograms were expanded at the same ratio to identify the trace methane impurity. The figures on the methane peak reflect the relative peak areas. The peak area corresponding to 10 ppb of methane standard in nitrogen was noticeable. In nitrogen and oxygen, the trace methane impurity was not detected (ND). However, the peak due to trace methane was observed in H_2, He and Ar. Approximately, those peak areas were smaller than one fifth of the peak area of 10 ppb methane standard. Anyway, the methane concentration in UHP gases was certainly less than 5 ppb.

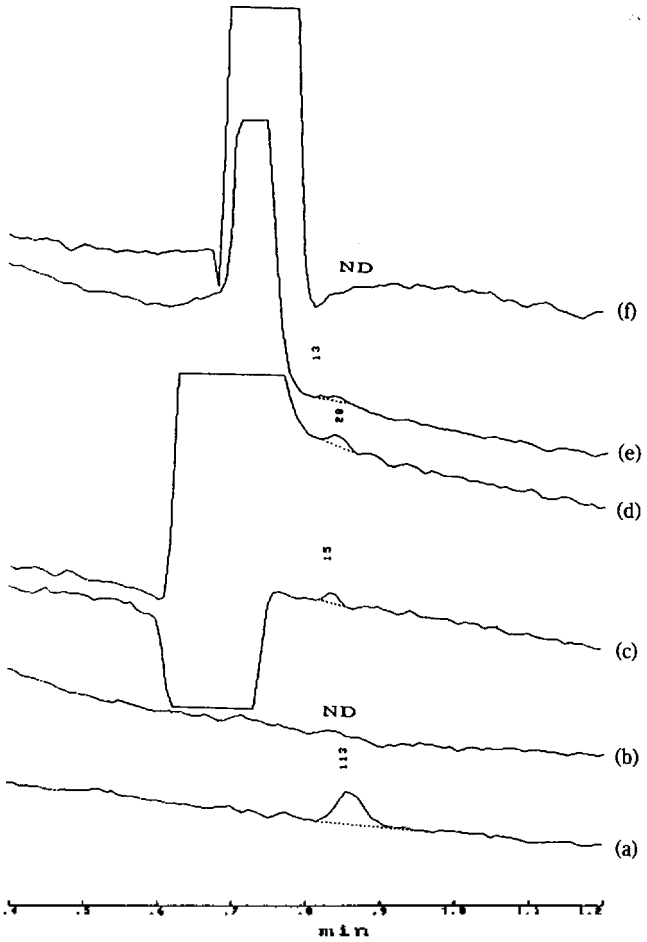

Figure 8. Chromatograms of UHP gases produced by DSSC: (a) 10 ppb of methane in N_2 (b) N_2 (c) He (d) H_2 (e) Ar, and (f) O_2.

In Figure 8, all but nitrogen showed the peak due to the matrix effect presented in our previous work,[13] because the carrier gas was nitrogen.

Conclusions

The trace methane impurity in UHP gases has been determined by GC-FID. GC-FID showed a linear response for methane impurity over a wide range of 10 to 10^4 ppb. The methane impurity concentration in UHP gases produced by DSSC were less than 5 ppb.

The LOD of FID for methane, by the IUPAC definition, is *ca.* 2.4 ppb. Therefore, it is possible to measure methane

impurity at levels as low as a few ppb.

References

1. Mitsui, Y.; Irie, T.; Mizakami, K. *Ultra Clean Technology* **1990**, 3.
2. Harata, K. A. *Market of the Electronic Industrial Gases and Chemicals*; Industrial Research Press: Tokyo, 1983.
3. Ronge, C.; Murphy, D. T.; Shadman, F. *Microcontamination Conf. Proc.* **1991**, 153.
4. Seksan Dheandhanoo; John G. Dulak; Jian Wei *Proc. Inst. Environ. Sci.* **1993**, 55.
5. Cowper, C. J.; DeRose, A. J. *The analysis of Gases by Chromatography*; Pergamon Press: Oxford, 1985.
6. McNair, H. M.; Bonelli, E. J. *Basic Gas Chromatogrphy*; Varian Aerograph: New York, 1960.
7. Ridgeway, R. G.; Ketkar, S. N.; Martinez de Pinillos *Microcontamination Conf. Proc.* **1992**, 392.
8. Maroulis, P. J.; Torres, A. L.; Bandy, A. R. *Geophysical Res. Lett.* **1977**, 510.
9. Long, G. L.; Winefordner, J. D. *Anal Chem.* **1983**, *55*(7), 712A.
10. Keith, L. H. *CHEMTECH Aug.* **1991**, 486.
11. Foley, J. P.; Dorsey, J. G. *Chromatographia* **1984**, *18*(9), 503.
12. Son, M. K.; Park, J. S.; Lee, I. S. *Morden Statistics*; Hakmoonsa: Seoul, 1977.
13. Son, M. R. ; Park, D. S. ; Kim, H. S. ; Park, B. E. *Hwahak Konghak* **1993**, *31*, 804.

Theoretical Studies on the Nonlinear Optical Properties of Conjugated Homologues of Hetero-TCNQ(X=O, S, Se)

U-Sung Choi*, Wang Ro Lee†, and Cheol-Ju Kim‡

**Department of Electronic Materials Engneering and †Department of Chemistry, Wonkwang University, Iri 570-749, Korea*

‡Department of Chemistry, Chonbuk National University, Chonbuk 560-756, Korea

Received May 17, 1994

A large number of π-conjugated polymers which exhibit fast response times and large optical nonlinearities have attracted much attention. It has been recognized that intramolecular electronic polarizations remakably contribute to the enhancement of nonlinear polarizabilities.[1-8] The conductive polymers, such as polyacethylene and polydiacetylenes, show the largest third-order nonlinear optical susceptibility $\chi^{(3)}$ among the organic materials. However, these values are too small to permit in the optical applications. Another possible origin of nonlinear optical polarizabilities in a supermolecular electronic polarization system have been studied by Meff *el al.*.[9] A supermolecular electronic polarization system has not yet been systemetically investigated. Organic charge transfer complexes systems, such as TXF−TCNQ(X=S, Se, Te), are well known for a supermolecular electronic polarization system. The extensively conjugated homologues of hetero-TCNQ(Figure 1, X=O, S, Se) have been attracted as potential electron acceptors for organic conductors. Thiophene- and selenophene-TCNQs were synthesized by Gronowitz and Uppstrom in 1974[10] and have been known as the first heteroquinonoid isologues of TCNQ. Figure 1 shows the hetero- TCNQ(X=O, S, Se) structures.

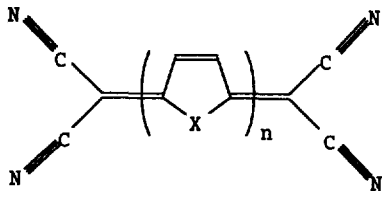

(a) X = S ; (b) X = O ; (c) X = Se

Figure 1. Structures of hetero-TCNQ(X=S, O, or Se).

Ab intio calculations of γ in the static field for regular polyenes have been carried out by Hurst *et al.*.[11] Zhao *et al.*[12] and Beljonne *et al.*[13] have demonstrated large third-order hyperpolarizabilities in thiophene oligomers. It has been reported that the mixed stack of tetracyanoquinodimethane (TCNQ) with perylene exhibits large γ values.[14]

In this study, frequency dependent nonlinear optical properties of conjugated homologues of hetero-TCNQ are calculated by the use of time-dependent Hartree-Fock mothods combined with semiempirical PM3[15] calculations. The hetero-TCNQ(X=O, S, Se) systems have planar structures with all quinoid structures. All the structures were fully optimized, and have all positive vibrational frequencies. Thus, at least, these should be at the local minima of the energy hypersurface.

In this study, the time-dependent Hartree-Fock treatment of nonlinear optical propeties for perturbations made up of a static electric field and an oscillating field presented Karna *et al.*[16] is used. The energy $E(E)$ of a molecular system perturbed by an external electric field E can be written as:

$$E(E)=E^0-\mu_a E^a-(2!)^{-1}\alpha_{ab}E^aE^b-(3!)^{-1}\beta_{abc}E^aE^b E^c-(4!)^{-1}\gamma_{abcd}E^aE^bE^cE^d-\cdots, \quad (1)$$

where the indices a, b, c, d, and so on indicate x, y, and z. In the above equation, μ_a is the a component of the dipole moment and α_{ab}, β_{abc}, and γ_{abcd} are the components of polarizability, second-order hyperpolarizability, and third-order hyperpolarizability tensors, respectively. A component of the total dipole moment P^a is obtained from the first derivative $(\partial E(E)/\partial E^a)$, so that from Eq. (1)

$$P^a=-\mu_a-\alpha_{ab}E^b-(2!)^{-1}\beta_{abc}E^bE^c-(3!)^{-1}\gamma_{abcd}E^bE^cE^d-\cdots \quad (2)$$

Hurst *et al.*[11] fitted the electronic properties as a function of the second order of n^{-1}. In this study, α, β, and γ values for infinitely long polymeric hetero cyclic rings are estimated by the following extrapolation procedure, as

$$\log A(n)=a_0+a_1/n+a_2/n^2+a_3/n^3, \quad (3)$$

where n is the number of the hetero cyclic ring unit and